ACS OMEGA

http://pubs.acs.org/journal/acsodf

Article

Oxidative-Extractive Desulfurization of Model Fuels Using a Pyridinium Ionic Liquid

Hanan Mohumed, Shofiur Rahman, Syed Ahmad Imtiaz, and Yan Zhang*

Cite This: *ACS Omega* 2020, 5, 8023−8031

Read Online

ACCESS | Metrics & More | Article Recommendations | Supporting Information

ABSTRACT: In this research, *N*-butyl-pyridinium tetrafluoroborate ([BPy][BF_4]) ionic liquid (IL) was synthesized and characterized by ^{1}H-NMR, ^{13}C-NMR, and FT-IR spectroscopy. The synthesized ionic liquid was employed as an extractive agent for the removal of dibenzothiophene (DBT), a typical organosulfur pollutant from the organic medium. The effect of extractive desulfurization on a model fuel with DBT was investigated. The impact of operating parameters, i.e., temperature, extraction time, IL-to-fuel ratio, and fuel to oxidizing agent ratio, on the extraction efficiency was investigated. It was observed that the IL to model fuel ratio and the H_2O_2 dosage have significant effects on desulfurization efficiency. An 89.49% DBT removal efficiency was obtained at a temperature of 30 °C after 35 min of extraction when the volume ratio of IL:model fuel:H_2O_2 was 1:1:0.04. A density functional theory (DFT) study was carried out to investigate the interactions between the IL and the sulfur-containing compounds DBT/$DBTO_2$.

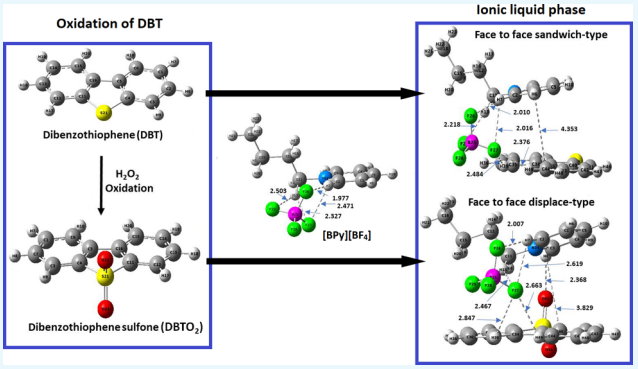

INTRODUCTION

Production of ultralow-sulfur or sulfur-free diesel fuel has become a major task of refineries all over the world.[1] As such, deep desulfurization and ultradeep desulfurization have become growing research areas and have attracted increasing attention. Hydrodesulfurization, a catalytic chemical process requiring the use of hydrogen to remove sulfur-containing compounds (S-compounds) from petroleum products, has the drawback of low efficiency in removing refractory S-compounds such as benzothiophene (BT), dibenzothiophene (DBT), and their alkyl derivatives. Alternative desulfurization processes, namely, oxidative desulfurization (ODS), extractive desulfurization (EDS), and bio-desulfurization, have recently been developed for deep desulfurization.[2,3] One environmental or "green" approach to remove refractory S-compounds that is quickly gaining in popularity is the use of ionic liquids (ILs) for EDS.[4] ILs are low-melting-point salts, typically with melting points below 100 °C. The cations of most ILs are organic-based moieties such as imidazolium, *n*-alkyl-pyridinium, tetraalkylammonium, and tetraalkylphosphonium ions, whereas their anionic counterparts can be organic or inorganic entities, such as halides, nitrate, acetate, hexafluorophosphate ([PF_6]), and tetrafluoroborate ([BF_4]).[5] Useful properties of ILs include low volatility, good thermal stability, controllable physicochemical properties, and long-term stability. Due to their unique properties, ILs have attracted great attention and have been increasing in use as green solvents for bioseparation, fuel desulfurization, and chemical synthesis.[6,7]

At the last count, more than a thousand ILs have been synthesized through various combinations of cations and anions, among which imidazolium or pyridinium-based ILs are mainly employed for desulfurization of fuels by EDS and oxidative-extractive desulfurization (OEDS). Utilizing 1-octyl-3-methylimidazolium tetrafluoroborate ([Omim][BF_4]) as an extractant, Alonso et al. achieved 87 wt % DBT and 79 wt % thiophene removals from a model fuel containing different hydrocarbons.[8] Chen et al. applied a Lewis acid IL, namely, 1-butyl-3-methylimidazolium chloride/$ZnCl_2$ ([Bmim][Cl]/$ZnCl_2$), during their experiments to extract DBT and thiophene from mixtures of hexane and octane. About 95.9% DBT removal and 93.8% thiophene removal were achieved at room temperature with a 1:1 (w/w) ratio of IL to oil in 30 min.[9] Zhu et al. prepared a temperature-responsive magnetic ionic liquid *N*-butyl-pyridinium tetrachloroferrate ([BPy]-[$FeCl_4$]) for desulfurization of DBT and BT from a model oil. They reported that 95.3% DBT removal and 75.0% BT removal were obtained in 10 min.[10] Wang et al. utilized six *n*-alkylpyridinium-based ILs for desulfurization of gasoline. Their

Received: January 8, 2020
Accepted: March 18, 2020
Published: April 2, 2020

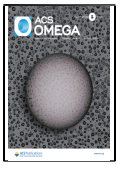

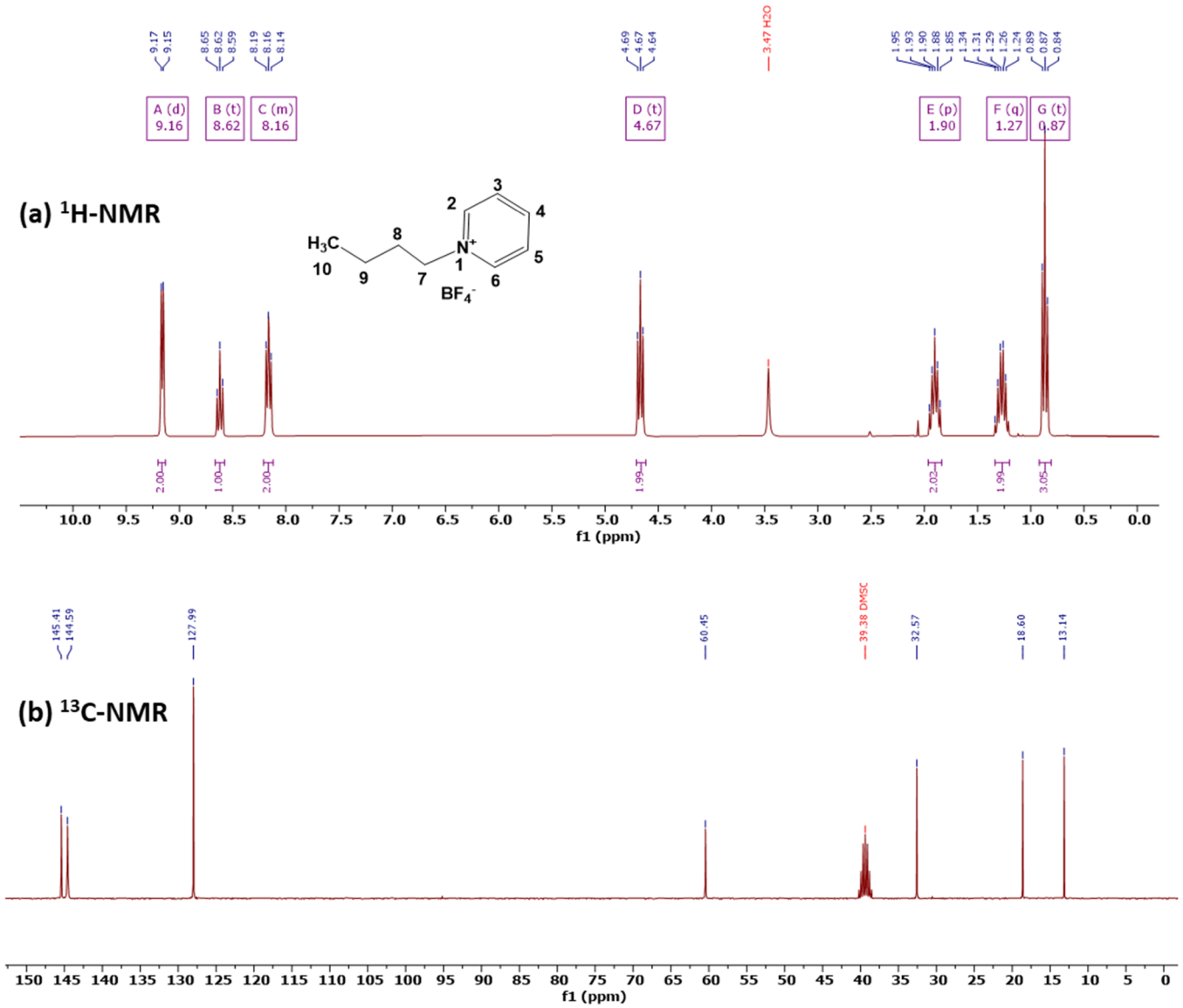

Figure 1. (a) ^{1}H-NMR (300 MHz, DMSO-d_6) and (b) ^{13}C-NMR (75 MHz, DMSO-d_6) spectra of [BPy][BF_4].

results indicated that [BPy][BF_4] has the highest sulfur removal efficiency under ambient conditions.[11]

The critical factors affecting the desulfurization efficiency of ILs are their size and structure. In experiments performed by Holbrey and co-workers, DBT was removed from dodecane via extraction through the application of ILs with different types of cations and anions.[12] By exposing DBT's partition ratio with ILs, the tests highlighted obvious differences within the cation types, adhering to the following order: dimethylpyridinium > methylpyridinium > pyridinium ≈ imidazolium ≈ pyrrolidinium. In related research inquiries, Gao et al. observed the following sequence efficiencies, i.e., [OPy][BF_4] > [HPy][BF_4] > [BPy][BF_4], for the removal of aromatic heterocyclic S-compounds from diesel with pyridinium ILs.[13] Similar observations were made by Wlazło and co-workers, who studied the extraction of thiophene and benzothiophene by 1-alkyl-cyanopyridinium bis{(trifluoromethyl)sufonyl}imide ILs.[14] They discovered that the solubility of aromatic S-compounds in ILs increases as the alkyl chain length of cations increases. This is because the induced polarity of the ring's π-electron cloud increases as the alky chain length becomes longer, leading to a stronger $\pi-\pi$ interaction between aromatic S-compounds and the imidazolium or pyridinium ring of ILs.

A big challenge for EDS using ILs is the coextraction of aromatic hydrocarbons. To counteract this inefficiency, oxidants are used together with ILs to increase the extraction selectivity of S-compounds. The use of ILs for catalysis was explored by Zhang et al. and Pârvulescu and Hardacre,[15,16] while Li et al. discussed the benefits of using ILs for green catalytic approaches.[17] Several other studies also looked at possible improvements to desulfurization methods.[18−20] These studies showed that the amount of aromatic S-compounds removed by OEDS increased by approximately 1 order of magnitude compared with EDS. This is because ILs not only serve as extractants of S-compounds but also provide suitable oxidation conditions for S-compounds to transform into sulfones and sulfur oxides. One of the most widely used oxidants for OEDS is hydrogen peroxide (H_2O_2) owing to its high oxygen content as well as, more recently, its green appeal. However, tests showed that excess H_2O_2 would be needed likely due to one of two reasons: (1) excess H_2O_2 prompts an equilibrium reaction, resulting in improved process efficiency,

https://dx.doi.org/10.1021/acsomega.0c00096
ACS Omega 2020, 5, 8023−8031

or (2) some catalysts incite decomposition of H_2O_2, leading to low utilization for oxidants.[20,21] In this regard, optimizing the operating conditions of the OEDS process to reduce the consumption of H_2O_2 is necessary.

Generally, employing ionic liquid for oxidative desulfurization can be beneficial on several different fronts, and the most important ones are optimal energy efficiency and ultralow sulfur levels in the end product. Another key advantage is the simplification of the overall process, which is accomplished by combining oxidation and extraction into a single stage. Despite many positive benefits of OEDS, some issues are still endemic to the procedure, and there is a lack of ionic liquid studies where most ILs have problems that make them impractical for mass implementation. The three main issues include high viscosity of ionic liquid, particularly amphiphilic (surfactant-inspired) ILs that are used to enable phase-transfer catalysis, high costs due to expensive anions and cations, and low efficiency in sulfur removal from real liquid fuels. These issues could potentially be resolved with further research and testing.[22,23]

In this work, a pyridinium-based IL *N*-butyl-pyridinium tetrafluoroborate ([BPy][BF_4]) was synthesized to investigate the oxidative desulfurization of DBT, an aromatic S-component comprising about 80% of total sulfur contents in diesel fuels. The focus of this investigation is to examine ways to optimize EDS and OEDS of DBT from a model fuel with *N*-butyl-pyridinium tetrafluoroborate ([BPy][BF_4]). To accomplish our research objective, a facile two-step synthetic process was employed to prepare [BPy][BF_4] followed by examining its structure by nuclear magnetic resonance (NMR) and Fourier transform infrared (FT-IR) spectroscopies. By studying the influences of different operating parameters, such as extraction time and temperature, the volume ratio of IL to model fuel, and dosage of the oxidant, the optimal extraction conditions were found. In order to reduce the operating cost, recovery of the IL from fuel desulfurization was also investigated. To better understand the extraction ability of the S-compound from the model fuel and to complement the experimental results, we investigated the interactions between DBT/$DBTO_2$ with ([BPy][BF_4] by density functional theory (DFT) calculations using the B3LYP/6-311++G(d,2p) level of theory. We believe that research outcomes of the current study will help to gain a better understanding of the role and key factors influencing the performance of ILs in desulfurization under moderate and environmentally friendly extraction conditions.

RESULTS AND DISCUSSION

^{1}H-NMR and ^{13}C-NMR Characterization of [BPy][BF_4]. The synthesized ionic liquid [BPy][BF_4] was analyzed by ^{1}H-NMR and ^{13}C-NMR, and the spectra are shown in Figure 1. The δ values of ^{1}H-NMR and ^{13}C-NMR of [BPy][BF4] in this work are consistent with those reported.[24,25] ^{1}H NMR (300 MHz, DMSO-d_6): δ = 9.13 (2H, d, J = 6.0 Hz, Py−$H_{(2,6)}$), 8.58 (1H, td, J = 7.9, 3.2 Hz, Py−H_4), 8.13 (2H, t, J = 6.5 Hz, Py−$H_{(3,5)}$), 4.63 (2H, td, J = 7.5, 2.0 Hz, Py−CH_2), 1.86 (2H, q, J = 7.4, Hz, Py−CH_2−CH_2), 1.24 (2H, m, J = 7.3, 2.0 Hz, CH_3−CH_2), and 0.84 (3H, td, −CH_3) ppm. ^{13}C NMR (75 MHz, DMSO-d_6): δ = 206.81, 149.06, 145.58, 144.24, 128.16, 60.64, 32.78, 30.67, 18.80, and 13.30 ppm.

Effect of Extraction Time. The effect of extraction time on the DBT removal rate was studied for ODS, EDS, and OEDS processes with an initial DBT concentration of 1000 ppm and IL to model fuel ratio of 1:1 to characterize the role of ionic liquid. As seen from Figure 2, approximately 10.0%

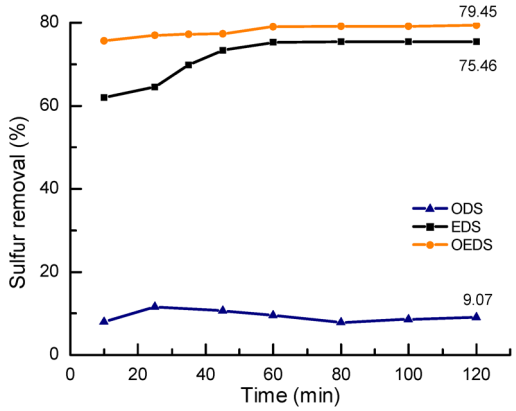

Figure 2. Desulfurization efficiency of ODS, EDS, and OEDS at different times ([DBT]$_{ini}$ = 1000 ppm, v(IL):v(oil) = 1:1, and T = 30 °C).

DBT was converted by H_2O_2 (4.0 vol %) in the absence of [BPy][BF_4] and/or extracting agent in the ODS experiment. The DBT removal rate by pure ionic liquid in the EDS process increases very fast with time within the first 45 min, while desulfurization efficiency increases slowly after 45 min and is nearly stable after 60 min, leading to a final DBT removal efficiency of 75.5%. Compared with ODS and EDS, the DBT removal rate by OEDS (addition of 0.1 vol % H_2O_2) is even faster under the same operating conditions, and the phase equilibrium can be reached after 60 min with an enhanced desulfurization efficiency of 79.5%.

Results from Figure 2 clearly show that [BPy][BF_4] acts as the extractant in both EDS and OEDS operations. In the OEDS process, extraction of DBT was accompanied by oxidation of DBT to its corresponding sulfoxide (DBTO) and sulfone ($DBTO_2$) due to the addition of the H_2O_2 oxidant. High polarity of the products (DBTO and $DBTO_2$) made them stay in the IL phase. As the concentration of DBT decreased in the IL phase, the extraction equilibrium was broken, and DBT was continuously extracted from oil phase to IL phase until reaction equilibrium was reached. However, complete conversion of DBT was not achieved due to the absence of acid catalysts. This experimental observation is consistent with previous research reports.[22,25]

Effect of Extraction Temperature. The reaction temperature plays a vital role in the OEDS process. The effect of temperature on DBT removal for the model fuel with different amounts of DBT was examined by varying the temperature from 20 to 40 °C, and the results are illustrated in Figure 3. Despite the different volume ratios of IL to model fuel used, higher desulfurization efficiency was observed at an elevated temperature. This is because the temperature has a direct effect on the kinetic rate constant, thereby increasing the rate of reaction and hence the removal rate of DBT. Not surprisingly, the desulfurization efficiency decreases when the volume ratio of IL to model fuel decreases as more amount of DBT makes the ionic liquid almost saturated. The highest DBT removal efficiencies obtained at 40 °C are 76.0, 71.5, and 68.9% when volume ratios of IL to model fuel are 1:1, 1:2, and 1:3, respectively.

https://dx.doi.org/10.1021/acsomega.0c00096
ACS Omega 2020, 5, 8023−8031

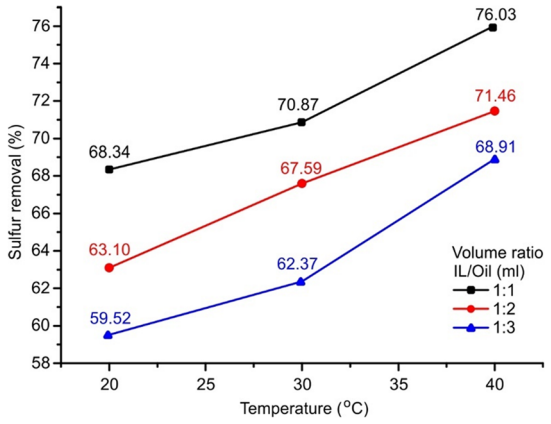

Figure 3. Oxidation extraction desulfurization efficiency at different temperatures ($[DBT]_{ini}$ = 1000 ppm, v(H_2O_2):v(oil) = 0.1%, and t = 40 min).

Effect of the Volume Ratio of IL to Model Fuel. The desulfurization efficiencies of EDS and OEDS for different volume ratios of IL to model fuel are depicted in Figure 4. For both operations, the desulfurization efficiency decreases when a lower volume ratio of IL to model fuel is used. The efficiency decreases from 89.5 to 75.4% for OEDS and 69.8 to 63.7% for EDS when the IL to model fuel ratio varies from 1:1 to 1:3, with all the other operating conditions being the same. In real applications, a proper volume ratio of IL to model fuel needs to be selected to balance the desulfurization efficiency and the treatment capacity.

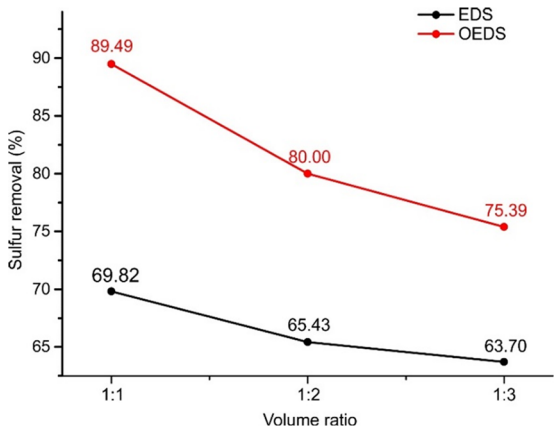

Figure 4. Desulfurization efficiency of EDS and OEDS at different volume ratios of IL to model fuel ($[DBT]_{ini}$ = 1000 ppm, v(H_2O_2):v(oil) = 4.0%, T = 30 °C, and t = 40 min).

Effect of the H_2O_2 Dosage. The influence of H_2O_2 dosage on desulfurization efficiency is shown in Figure 5. It is obvious that the desulfurization efficiency increases with increasing amount of H_2O_2 added to the system. However, the influence of H_2O_2 dosage (characterized by the volume ratio of H_2O_2 to model fuel) is slightly different when different volume ratios of IL to model fuel are applied. At a high volume ratio (1:1) of IL to model fuel, only 0.1 vol % H_2O_2 present in the system led to a 7.16% increase in desulfurization efficiency from 69.82 (without using H_2O_2) to 77.0%, and a further increase of 4.3% in desulfurization efficiency was obtained, with 1.0 vol % H_2O_2 being used. In the case of a low volume ratio (1:4) of IL to model fuel, desulfurization efficiency increased slightly from

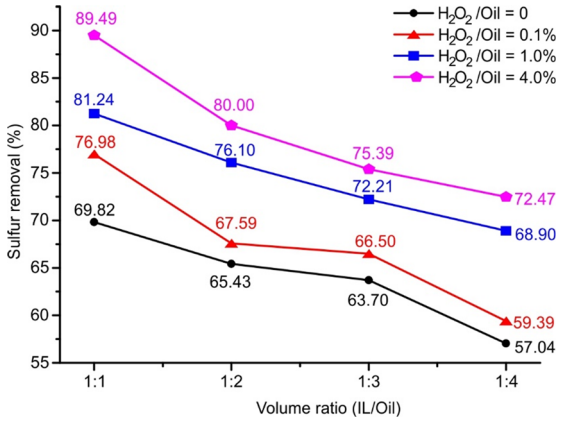

Figure 5. Desulfurization efficiency of EDS and OEDS at different volume ratios of H_2O_2 to model fuel ($[DBT]_{ini}$ = 1000 ppm, T = 30 °C, and t = 40 min).

57.0 (without using H_2O_2) to 59.4% after adding 0.1 vol % H_2O_2. However, a remarkable increase of 9.5% in desulfurization efficiency was obtained, with 1.0 vol % H_2O_2 being used. The maximum desulfurization efficiency for different volume ratios of IL to model fuel was achieved when an extra amount of H_2O_2 (4.0 vol %) is used.

Table 1 compares the desulfurization performance of $[BPy][BF_4]$ in the present work with those of other pyridinium-based ionic liquids reported previously.[10,15,24,26,27] Ionic liquid $[CH_2COOHPy][HSO_4]$ is capable of completely removing DBT from model fuel due to the presence of the carboxyl group in its alkyl chain. This ionic liquid works as both catalyst and extractant in the OEDS process. Other pyridinium-based ionic liquids mainly serve as extractants; thus, they are not able to remove DBT completely. Desulfurization performance of $[BPy][BF_4]$ in this work is competitive with those listed in Table 1.

Regeneration of the Ionic Liquid. The regeneration and subsequent recycling of ILs are greatly important in industrial applications. In this work, the S-loaded ionic liquid was regenerated by distillation first to remove water and H_2O_2 followed by re-extraction using CCl_4. The regenerated IL was analyzed by NMR spectroscopy (Supporting Information, Figures S1 and S2), which indicated that there was no change in the structure of the regenerated $[BPy][BF_4]$.

The regenerated IL was reused for OEDS of DBT under the optimized conditions for eight consecutive cycles, and the results of DBT removal efficiency are demonstrated in Figure 6. Although the extraction efficiency of regenerated IL slightly declines after each cycle, the DBT removal efficiency is still quite high after the 8th cycle. A similar observation was reported by Zhao et al. using the same ionic liquid.[24] Nevertheless, due to the high energy cost of distillation, this method is only suitable on the laboratory scale. Alternative low-energy-cost regeneration techniques need to be investigated for large-scale applications.

Desulfurization of DBT from Diesel Fuel with $[BPy][BF_4]$. In the present study, real diesel fuel containing 1000 ppm DBT was treated with $[BPy][BF_4]$ to test its extraction ability from real hydrocarbon feedstock. The oxidative-extraction of DBT from diesel were conducted at 40 ° C with a fixed volume ratio (1:1) of IL to diesel fuel and H_2O_2 dosage (4.0 vol %). It can be seen from Figure 7 that the DBT removal rate from diesel is lower than that from the model oil

https://dx.doi.org/10.1021/acsomega.0c00096
ACS Omega 2020, 5, 8023−8031

Table 1. DBT Removal Efficiency by the OEDS Process Using Pyridinium-Based Ionic Liquids

ionic liquid	$[DBT]_{ini}$	temp. and time	$n(H_2O_2)/n(DBT)$	DBT removal	ref
$[BPy][FeCl_4]$	500 ppm	40 °C, 10 min	8:1	95.3%	10
$[CH_2COOHPy][HSO_4]$	1000 ppm	30 °C, 60 min	6:1	99.9%	15
$[BPy][BF_4]$	1000 ppm	30 °C, 30 min	720:1	74.0%	24
$[BPy][BF_4]$	1000 ppm	40 °C, 60 min	not reported	82.1%	26
[BPy][SCN]	1000 ppm	40 °C, 60 min	not reported	84.5%	26
$[BPy][H_2PO_4]$	1000 ppm	40 °C, 60 min	not reported	88.3%	26
$[C_4^3Py][FeCl_4]$	1000 ppm	25 °C, 20 min	6:1	85.6%	27
$[BPy][BF_4]$	1000 ppm	30 °C, 40 min	18:1	81.2%	this work
$[BPy][BF_4]$	1000 ppm	30 °C, 40 min	72:1	89.5%	this work

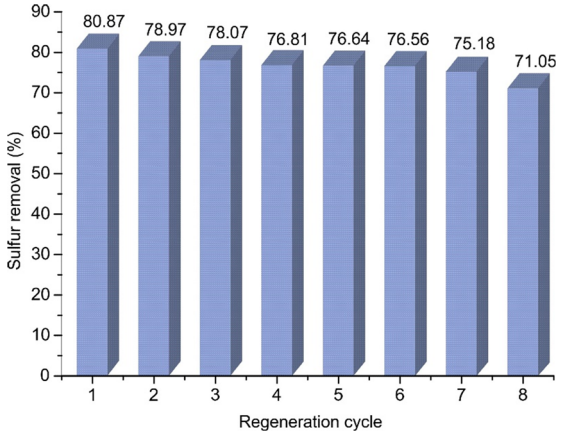

Figure 6. OEDS of DBT by regenerated $[BPy][BF_4]$ ($[DBT]_{ini}$ = 1000 ppm, v(IL):v(oil) = 1:1, $v(H_2O_2)$:v(oil) = 4.0%, and T = 30 °C).

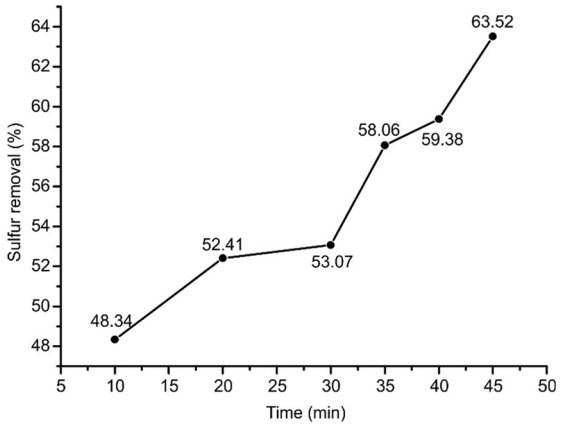

Figure 7. Desulfurization efficiency of DBT in diesel fuel ($[DBT]_{ini}$ = 1000 ppm, v(IL):v(oil) = 1:1, $v(H_2O_2)$:v(oil) = 4.0%, and T = 40 °C).

by $[BPy][BF_4]$. The reduced DBT removal rate by $[BPy][BF_4]$ from diesel is mainly due to the existence of aromatic hydrocarbons in diesel. GC−MS analysis of diesel fuel indicates that paraffin constituents range from C_8H_{18} to $C_{20}H_{42}$, and there are about 20 mol % aromatic hydrocarbons in diesel. Compared with hexane (model fuel), aromatic hydrocarbons have strong interactions with IL, and hence, they are partially miscible in IL, which reduces the selectivity of $[BPy][BF_4]$ to DBT.

DFT Study. The energetically most stable optimized structures of the $[BPy][BF_4]$, DBT, $DBTO_2$, and their corresponding complexes ($[BPy][BF_4]$)⊃DBT and ($[BPy][BF_4]$)⊃$DBTO_2$ are shown in Figure 8. The calculated interaction energies are summarized in Table 2.

As illustrated in Figure 8, the ionic liquid $[BPy][BF_4]$ contains a pyridine ring, which has $\pi-\pi$ interactions with both DBT and $DBTO_2$. Non-covalent weak interactions such as $\pi-\pi$ interactions, electrostatic interactions, weak hydrogen bonding, and hydrophobic lipophilic interactions play important roles in supramolecular chemistry.[28,29] Non-covalent interactions could be the best possible mechanisms for the extraction of the sulfur-containing compounds from the model fuel by the pyridinium-based IL. Aromatic−aromatic interactions ($\pi-\pi$ stacking) are generally defined as the attractive noncovalent interactions that occur between the-electronic clouds of aromatic systems in *parallel*, *face-to-face*, or *edge-to-face* orientation interactions.[30−33] Hohenstein and Sherrill investigated the effects of heterocyclic aromatic atoms in various configurations of a pyrimidine−benzene complex for their $\pi-\pi$ stacking interactions.[33] They reported that the presence of an electronegative nitrogen heteroatom into an aromatic ring has large effects on similar *stacked*, *parallel-displaced*, and *T-shaped* dimers. Figure 8 shows the most stable optimized structures of the ($[BPy][BF_4]$)⊃DBT/$DBTO_2$ complexes. There are two types of possible $\pi-\pi$ interactions found between $[BPy][BF_4]$ and DBT, resulting in the formation of complexes with *face-to-face parallel-sandwich* (Figure 8c) and *edge-tilted-T-shaped* (Figure 8e) geometries. On the other hand, the $\pi-\pi$ interactions between $[BPy][BF_4]$ and $DBTO_2$ lead to *face-to-face parallel-displaced* (Figure 8d) and *edge-tilted-T-shaped* (Figure 8f) structures.

The nitrogen atom of the pyridine ring in the ionic liquid draws electrons away from the ring carbon atoms inductively, thereby increasing the positive charges of the pyridinium hydrogen atoms, thus making the pyridine moiety more effective as a "π-hydrogen bond" donor. In the *face-to-face parallel-sandwich* type interaction ($[BPy][BF_4]$)⊃DBT as shown in Figure 8c, the pyridinium hydrogens form three hydrogen bonds (C2−H7···F26, C2−H7···F27, and C11−H13···F29), and their bond distances are 2.010, 2.616, and 2.218 Å, respectively. One of the other pyridinium C−H···π-interactions with DBT, particularly PyC1−H6···C44 (DBT) has a distance of 4.353 Å and is almost parallel to the DBT plane, making it possible to form the "sandwich" type arrangement. Meanwhile, the anion BF_4^- and DBT form weak hydrogen bonding, the bond distances of DBT−C34−H39···F27 and DBT−C44−H49···F27 are 2.484 and 2.376 Å, respectively.

In the *edge-tilted-T-shaped* structure shown in Figure 8e, the pyridinium hydrogens form three hydrogen bonds (C2−H7···F26, C2−H7···F27, and C11−H13···F27), with bond distances of 2.019, 2.519, and 2.187 Å, respectively. One of the other

https://dx.doi.org/10.1021/acsomega.0c00096
ACS Omega 2020, 5, 8023−8031

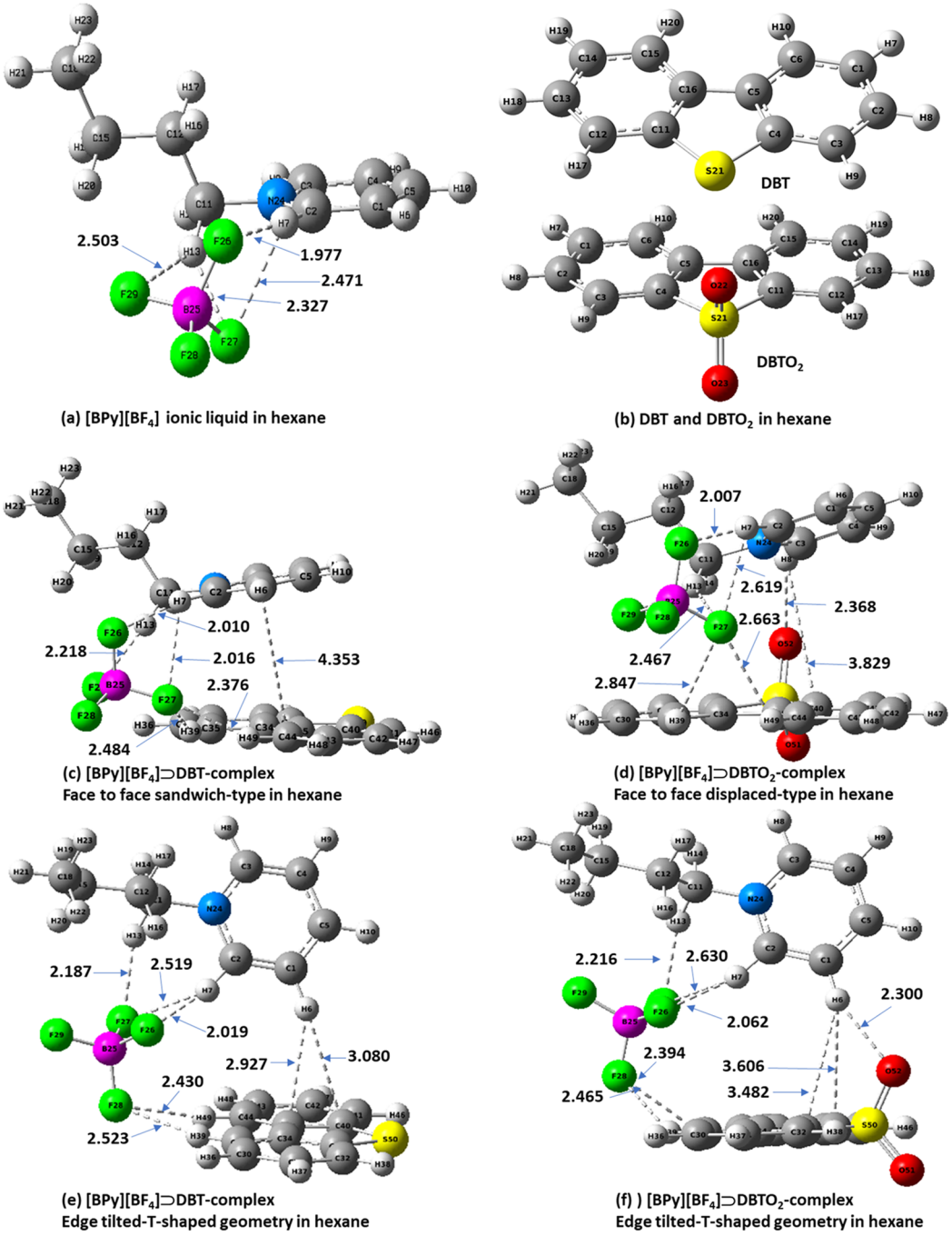

Figure 8. Geometry optimized structures of (a) [BPy][BF_4], (b) dibenzothiophene (DBT), dibenzothiophene sulfone ($DBTO_2$), (c,e) ([BPy][BF_4])⊃DBT, and (d,f) ([BPy][BF_4])⊃$DBTO_2$ in hexane. Color code: carbon = gray; hydrogen = white; nitrogen = blue; oxygen = red; sulfur = yellow, boron = magenta; fluorine = green.

pyridinium C−H···π interactions with DBT, particularly PyC1−H6, which is almost perpendicular to the DBT plane, makes it possible to form the "T-shaped" type arrangement. The PyC1−H6···C33−DBT and PyC1−H6···C34−DBT bond distances are 2.927 and 3.080 Å, respectively. The BF_4^- anion and DBT form weak hydrogen bonding, and bond distances of DBT−C34−H39···F28 and DBT−C44−H49···F28 are 2.523 and 2.430 Å, respectively. The position of the BF_4^- anion is above the side of the pyridinium and DBT plane in the ([BPy][BF_4])⊃DBT complex, which therefore creates less steric inhibition between the pyridinium and DBT for both *sandwich* and *T-shaped* type arrangements. The interaction energies of ([Bpy][BF_4])⊃DBT for *sandwich* and *T-shaped* geometries are −28.99 and −27.66 kJ·mol^{-1} in the gas-phase calculations, −16.48 and −16.15 kJ·mol^{-1} in the hexane solvent system, and −14.37 and −14.69 kJ·mol^{-1} in the CCl_4 solvent system, respectively.

The $\pi-\pi$ interactions between [BPy][BF_4] and $DBTO_2$, namely, *face-to-face parallel-displaced* and *edge-tilted-T-shaped*, can be seen in Figure 8d,f, respectively. In the *face-to-face parallel-displaced* interaction for ([BPy][BF_4])⊃$DBTO_2$ (Figure 8d), the pyridinium hydrogens form four hydrogen bonds (C2−H7···F26, C2−H7···F27, C11−H13···F29, and C3−H8···O52), and the bond distances are 2.007, 2.619, 2.467, and

https://dx.doi.org/10.1021/acsomega.0c00096
ACS Omega 2020, 5, 8023−8031

Table 2. Calculated Interaction Energies (ΔIE kJ/mol) for the Ionic Liquid [BPy][BF_4] with DBT and $DBTO_2$ Sulfur-Containing Compounds in Model Fuel (Hexane) and CCl_4 Solvent Systems

compound	ΔIE, kJ/mol		
	gas phase	hexane	CCl_4
[BPy]⊃[BF_4]	−336.97	−175.78	−148.43
([BPy][BF_4])⊃DBT *face to face parallel sandwich*	−28.98	−16.48	−14.37
([BPy][BF_4])⊃$DBTO_2$ *face to face parallel-displaced*	−50.26	−31.16	−29.07
([BPy][BF_4])⊃DBT *edge-tilted-T-shaped*	−27.66	−16.15	−14.69
([BPy][BF_4])⊃$DBTO_2$ *edge-tilted-T-shaped*	−51.63	−32.67	−28.91

2.514 Å, respectively. For one of the other pyridinium C−H···π interactions with $DBTO_2$, i.e., PyC3−H8···C40 ($DBTO_2$), the bond distance is 3.829 Å, which is almost parallel to the $DBTO_2$ plane, making it possible to form the *face-to-face parallel-displaced*-type arrangement. The anion [BF_4] and $DBTO_2$ form weak hydrogen bonding, with the distances of $DBTO_2$−C34−H39···F27 and $DBTO_2$−C44−H49···F27 being 2.847 and 2.663 Å, respectively.

In the *edge-tilted-T-shaped* interaction for ([BPy][BF_4])⊃$DBTO_2$ (Figure 8f), pyridinium hydrogens form four hydrogen bonds (C2−H7···F26, C2−H7···F27, C11−H13···F27, and C3−H8···O52), and the distances are 2.062, 2.630, 2.216, and 2.300 Å, respectively. The other pyridinium C−H···π interactions with $DBTO_2$, particularly C1−H6···C33 and C1−H6···C40 interactions, which are almost perpendicular to the $DBTO_2$ plane, make it possible to form the *T-shaped* arrangement. The PyC1−H6···C33−$DBTO_2$ and PyC1−H6···C40−DBT bond distances are 3.606 and 3.482 Å, respectively. The anion BF_4^- and $DBTO_2$ show weak hydrogen bonding, distances of 2.465 and 2.349 Å, respectively, for DBT−C44−H39···F28 and $DBTO_2$−C35−H49···F28. The position of the BF_4^- anion is above one side of the pyridinium and $DBTO_2$ plane in the ([BPy][BF_4])⊃$DBTO_2$, which thus creates less steric inhibition between the pyridinium and $DBTO_2$ for both the *parallel-displaced* and *T-shaped* geometry structures. The interaction energies of ([BPy][BF_4])⊃$DBTO_2$ for *sandwich* and *T-shaped* geometries are −50.26 and −51.63 kJ·mol^{-1} in the gas-phase calculations, −31.16 and −32.767 kJ·mol^{-1} in the hexane solvent system, −29.07 and −28.91 kJ·mol^{-1} in the CCl_4 solvent system, respectively. The hydrogen bonding between the oxygen atom (S=O) of the $DBTO_2$ with the pyridinium hydrogen (C1−H6···O52, 2.300 Å) and higher polarity of the $DBTO_2$ could be the possible reasons for the higher interaction energies of ([BPy][BF_4])⊃$DBTO_2$ versus those of ([BPy][BF_4])⊃DBT. The dipole moments of $DBTO_2$ and DBT are 6.699 and 0.869 D, respectively, in the hexane solvent system. Due to the higher polarity of the $DBTO_2$, it is more likely to be solubilized in the ionic-liquid phase rather than the model-fuel phase based upon these calculations. The interaction energies of the [BPy][BF_4] complexes with DBT and $DBTO_2$ decrease in the hexane and CCl_4 solvent systems compared with those of gas-phase calculations. To get a better insight of the solvation effect for regeneration of the ionic liquid from the ionic-liquid-mediated desulfurization process, further experimental and computational studies with different solvent systems are underway.

CONCLUSIONS

A pyridinium-based ionic liquid [BPy][BF_4] was synthesized by a two-step method and was characterized by ^{1}H-NMR, ^{13}C-NMR, and FT-IR spectroscopy. The NMR and IR spectra confirmed the molecular structure and configuration of [BPy][BF_4]. The prepared ionic liquid was then used as an extractant to remove dibenzothiophene (DBT) from a model fuel under different experimental conditions. [BPy][BF_4] was found to be effective in the extraction of DBT from the model fuel as both EDS and OEDS were complete within 1 h. The results indicate that H_2O_2 dosage and volume ratio of IL to model fuel have a significant impact and interplay on desulfurization efficiency. Desulfurization efficiency increased remarkably with increasing amount of H_2O_2 when a high volume ratio (1:1) of IL to model fuel is used. Nonetheless, a gradual increase of DBT removal efficiency is observed with increasing dosage of H_2O_2 when a low volume ratio of IL to model fuel is applied. In addition, our experimental results confirmed that [BPy][BF_4] can be regenerated and reused without a significant decline in desulfurization efficiency. The DFT calculation analysis shows that the interaction energies for ([BPy][BF_4])⊃$DBTO_2$ (−51.63, −32.67, and −28.91 kJ·mol^{-1}) are almost 2 times higher than those for ([BPy][BF_4])⊃DBT (−27.66, −16.15, and −14.69 kJ·mol^{-1}) in the gas phase, hexane, and CCl_4 solvent systems, respectively. These results strongly suggest that the π−π interaction and hydrogen bonds (F···H and O···H) play important roles for the interaction of the ionic liquid [BPy][BF_4] with DBT/$DBTO_2$. The DFT-calculated interaction energies between [BPy][BF_4] and DBT/$DBTO_2$ strongly support our experimental results. The DFT calculation results imply that the oxidative desulfurization is necessary to increase the removal efficiency of DBT from fuels.

EXPERIMENTAL AND CALCULATION METHODS

Synthesis of *N*-Butyl-pyridinium Tetrafluoroborate Ionic Liquid ([BPy][BF_4]). The ionic liquid ([BPy][BF_4]) was synthesized according to the reported procedures.[24,25] *N*-Butyl-pyridinium bromide was first synthesized by the following procedure: A solution of pyridine (40.2 mL, 0.50 mol) and 1-bromobutane (53.9 mL, 0.50 mol) was added into a solution of cyclohexane (50 mL) in a 250 mL round-bottom flask connected to a water-cooled reflux condenser fitted with an anhydrous calcium chloride drying tube. The reaction mixture was stirred by a magnetic stirrer at 64 °C for 24 h until no more precipitate formed. The white precipitate was filtered off, and then unreacted pyridine was removed from the resulting solid by washing with ethyl acetate (3 × 50 mL). The resulting solid was evaporated in a vacuum drying oven to remove the remaining ethyl acetate to yield *N*-butyl-pyridinium bromide (73.1 g, 67.7%) as a colorless solid.

In the second step, the freshly synthesized *N*-butyl-pyridine bromide (64.8 g, 0.30 mol) was mixed with potassium tetrafluoroborate (44 g, 0.30 mol). The solid mixture was dissolved in 300 mL of acetone in a 500 mL conical flask, and the reaction mixture was stirred by a magnetic stirrer at room temperature for 24 h. The solution was then placed into a refrigerator for 24 h until potassium bromide (KBr) precipitated from the solution. Then the resulting precipitate was filtered off, and the solvent was removed by rotary evaporation to yield *N*-butyl-pyridinium tetrafluoroborate

https://dx.doi.org/10.1021/acsomega.0c00096
ACS Omega 2020, 5, 8023−8031

$[BPy][BF_4]$ ionic liquid (12.4 g) as a yellowish liquid. The ionic liquid was stored in a fridge for further use.

Extractive and Oxidative-Extractive Desulfurization Experiments. The model fuel was employed as a surrogate for real fuel with an initial DBT concentration of 1000 ppm by dissolving 0.50 g of DBT in 500 mL of *n*-hexane. EDS experiments were conducted in 50 mL glass conical flasks. The volume ratios of the ionic liquid to model fuel were 1:1, 1:2, 1:3, and 1:4. Different amounts of ionic liquid were added to the model fuel, and the mixtures were magnetically stirred vigorously at 30 °C with various extraction times. The two layers were separated after completion of the reaction and settling of the reaction mixture. The S-content of the upper phase (model fuel phase) was analyzed by UV−vis spectroscopy at λ_{max} 284 nm. The desulfurization efficiency is presented in terms of the S-removal based on the initial and final S-contents in the model fuel via the following equation:

$$\eta = \frac{[DBT]_{ini} - [DBT]_{final}}{[DBT]_{ini}} \times 100 \quad (1)$$

The ODS test was performed by mixing 10 mL of model fuel and 4.0 vol % hydrogen peroxide (H_2O_2, 30 wt %) at 30 °C under constant stirring. A solution of the model fuel (10.0 mL) was mixed with the ionic liquid and H_2O_2 for OEDS experiments. The resulting mixtures with different volume ratios among ionic liquid, model fuel, and oxidant agent were stirred under various temperatures (20, 30, and 40 °C) and extraction time periods. The aqueous phase was separated from the oil phase using a separatory funnel. Samples were collected from both phases for analysis to define the oxidation extraction desulfurization efficiency.

Recycling of Ionic Liquid. Regeneration of the S-loaded ionic liquid was conducted by distillation in an oil bath at 110 °C to remove H_2O_2 followed by re-extraction using tetrachloromethane (CCl_4) at 30 °C for 30 min by using an incubator shaker (New Brunswick Scientific, Innova 43), with a volume ratio of ionic liquid to tetrachloromethane being 1:1. The mixture was left to stand for 10 min for the phases to separate. The lower layer is a mixture of CCl_4 and dibenzothiophene, and the upper layer is the regenerated ionic liquid. The regenerated ionic liquid was analyzed by ^{1}H-NMR, ^{13}C-NMR, and FT-IR spectroscopy for its purity.

Analytical Methods. The synthesized ionic liquid product ($[BPy][BF_4]$) was characterized by NMR and IR analyses. The ^{1}H-NMR and ^{13}C-NMR NMR spectra of $[BPy][BF_4]$ were recorded on a Bruker Avance 300 MHz spectrometer. Dimethyl sulfoxide (DMSO) was used as the solvent.

Oil-phase samples from EDS and OEDS processes were analyzed by an Agilent Cary 6000i UV−vis−IR spectrophotometer at a wavelength of λ_{max} 284 nm to determine DBT concentration. Standard solutions with DBT concentrations of 50, 30, 20, 15, 10, 7, and 5 ppm in *n*-hexane were used to get the calibration curve.

An Agilent HPLC 1260 Infinity II was used for the quantitative assay of DBT in the oil phase from the ODS test. The system was equipped with a quaternary pump, an autosampler, a Zorbax XDB-C18 column (4.6 × 250 mm, 5 μm), and a diode array UV detector. The mobile phase was 90% methanol in 10% water (v/v, %) with a flow rate of 1.0 mL/mm. The wavelength of UV was set at 284 nm. For the quantification of DBT, the external standards with DBT contents of 500, 400, 300, 200, and 100 ppm were used to get the calibration curve.

DFT Calculations. To better understand the interactions of sulfur-containing compounds dibenzothiophene (DBT) and dibenzothiophene sulfone ($DBTO_2$) with *N*-butyl-pyridinium tetrafluoroborate ionic liquid ($[BPy][BF_4]$), a quantum chemical density functional theory (DFT) calculation was carried out. Our primary purpose in this work is to evaluate the experimental extraction efficiency results with calculated DFT interaction energies of the DBT/$DBTO_2$ by $[BPy][BF_4]$. All the computational calculations were carried out with Gaussian 09.[34] The geometries of all the structures were fully optimized at the B3LYP/6-311++G(d,2p) level of theory in the gas phase, hexane, and CCl_4 solvent systems using the polarized continuum model (PCM). The structures of *N*-butyl-pyridinium cation [BPy] interacting with the tetrafluoroborate anion $[BF_4]$ at different binding sites were first optimized, and the most stable structure of the $[BPy][BF_4]$ was selected. The stable optimized structure of $[BPy][BF_4]$ was further optimized with DBT and $DBTO_2$ at different binding sites. The interaction energies between the ILs and DBT/$DBTO_2$ are defined as follows:

$$\Delta IE = E_{[BPy]\supset[BF_4]} - (E_{([BPy])} + E_{([BF_4])}) \quad (2)$$

$$\Delta IE = E_{([BPy][BF_4])\supset DBT/DBTO_2} - (E_{[BPy][BF_4]} + E_{[DBT/DBTO_2]}) \quad (3)$$

■ ASSOCIATED CONTENT

Supporting Information

The Supporting Information is available free of charge at https://pubs.acs.org/doi/10.1021/acsomega.0c00096.

NMR and FT-IR spectra of the synthesized $[BPy][BF_4]$ and DFT calculation results (PDF)

■ AUTHOR INFORMATION

Corresponding Author

Yan Zhang − *Faculty of Engineering and Applied Science, Memorial University of Newfoundland, St. John's, NL A1B 3X5, Canada;* orcid.org/0000-0003-0107-1014; Email: yanz@mun.ca

Authors

Hanan Mohumed − *Faculty of Engineering and Applied Science, Memorial University of Newfoundland, St. John's, NL A1B 3X5, Canada*

Shofiur Rahman − *Aramco Laboratory for Applied Sensing Research, King Abdullah Institute for Nanotechnology, King Saud University, Riyadh 11451, Saudi Arabia*

Syed Ahmad Imtiaz − *Faculty of Engineering and Applied Science, Memorial University of Newfoundland, St. John's, NL A1B 3X5, Canada;* orcid.org/0000-0002-2715-9084

Complete contact information is available at: https://pubs.acs.org/10.1021/acsomega.0c00096

Notes

The authors declare no competing financial interest.

■ ACKNOWLEDGMENTS

H.M. is grateful to the Ministry of Libyan Government for providing financial support during her postgraduate study at

Memorial University of Newfoundland. Support and assistance in this study from Memorial University of Newfoundland and Compute Canada are greatly acknowledged.

REFERENCES

(1) Kulkarni, P. S.; Afonso, C. A. M. Deep desulfurization of diesel fuel using ionic liquids: current status and future challenges. *Green Chem.* **2010**, *12*, 1139−1149.
(2) Dharaskar, S. A.; Wasewar, K. L.; Varma, M. N.; Shende, D. Z.; Yoo, C. Synthesis, characterization and application of 1-butyl-3-methylimidazolium tetrafluoroborate for extractive desulfurization of liquid fuel. *Arab. J. Chem.* **2016**, *9*, 578−587.
(3) Ibrahim, M. H.; Hayyan, M.; Hashim, M. A.; Hayyan, A. The role of ionic liquids in desulfurization of fuels: A review. *Renewable Sustainable Energy Rev.* **2017**, *76*, 1534−1549.
(4) Kianpour, E.; Azizian, S.; Yarie, M.; Zolfigol, M. A.; Bayat, M. A task-specific phosphonium ionic liquid as an efficient extractant for green desulfurization of liquid fuel: An experimental and computational study. *Chem. Eng. J.* **2016**, *295*, 500−508.
(5) Plechkova, N. V.; Seddon, K. R. Applications of ionic liquids in the chemical industry. *Chem. Soc. Rev.* **2008**, *37*, 123−150.
(6) Vekariya, R. L. A review of ionic liquids: Applications towards catalytic organic transformations. *J. Mol. Liq.* **2017**, *227*, 44−60.
(7) Moghadam, F. R.; Azizian, S.; Bayat, M.; Yarie, M.; Kianpour, E.; Zolfigol, M. A. Extractive desulfurization of liquid fuel by using a green, neutral and task specific phosphonium ionic liquid with glyceryl moiety: A joint experimental and computational study. *Fuel* **2017**, *208*, 214−222.
(8) Alonso, L.; Arce, A.; Francisco, M.; Rodriguez, O.; Soto, A. Gasoline desulfurization using extraction with $[C_8mim][BF_4]$ ionic liquid. *AIChE J.* **2007**, *53*, 3108−3115.
(9) Chen, X.; Yuan, S.; Abdeltawab, A. A.; Al-Deyab, S. S.; Zhang, J.; Yu, L.; Yu, G. Extractive desulfurization and denitrogenation of fuels using functional acidic ionic liquids. *Sep. Purif. Technol.* **2014**, *133*, 187−193.
(10) Zhu, W.; Wu, P.; Yang, L.; Chang, Y.; Chao, Y.; Li, H.; Jiang, Y.; Jiang, W.; Xun, S. Pyridinium-based temperature-responsive magnetic ionic liquid for oxidative desulfurization of fuels. *Chem. Eng. J.* **2013**, *229*, 250−256.
(11) Wang, J.-l.; Zhao, D.-s.; Zhou, E.-p.; Dong, Z. Desulfurization of gasoline by extraction with N-alkyl-pyridinium-based ionic liquids. *J. Fuel Chem. Technol.* **2007**, *35*, 293−296.
(12) Holbrey, J. D.; López-Martin, I.; Rothenberg, G.; Seddon, K. R.; Silvero, G.; Zheng, X. Desulfurisation of oils using ionic liquids: selection of cationic and anionic components to enhance extraction efficiency. *Green Chem.* **2008**, *10*, 87−92.
(13) Gao, H.; Luo, M.; Xing, J.; Wu, Y.; Li, Y.; Li, W.; Liu, Q.; Liu, H. Desulfurization of fuel by extraction with pyridinium-based ionic liqiuds. *Ind. Eng. Chem. Res.* **2008**, *47*, 8384−8388.
(14) Wlazło, M.; Ramjugernath, D.; Naidoo, P.; Domańska, U. Effect of the alkyl side chain of the 1-alkylpiperidinium-based ionic liquids on desulfurization of fuels. *J. Chem. Thermodyn.* **2014**, *72*, 31−36.
(15) Zhang, C.; Pan, X.; Wang, F.; Liu, X. Extraction-oxidation desulfurization by pyridinium-based task-specific ionic liquids. *Fuel* **2012**, *102*, 580−584.
(16) Pârvulescu, V. I.; Hardacre, C. Catalysis in ionic liquids. *Chem. Rev.* **2007**, *107*, 2615−2665.
(17) Li, F.-T.; Wu, B.; Liu, R.-H.; Wang, X.-J.; Chen, L.-J.; Zhao, D.-S. An inexpensive N-methyl-2-pyrrolidone-based ionic liquid as efficient extractant and catalyst for desulfurization of dibenzothiophene. *Chem. Eng. J.* **2015**, *274*, 192−199.
(18) Elwan, H. A.; Zaky, M. T.; Faray, A. S.; Soliman, F. S.; Hassan, M. E. D. A coupled extractive-oxidative process for desulfurization of gasoline and diesel fuels using a bifunctional ionic liquid. *J. Mol. Liq.* **2017**, *248*, 549−555.
(19) Choi, A. E. S.; Roces, S.; Dugos, N.; Wan, M.-W. Oxidation by H_2O_2 of bezothiophene and dibenzothiophene over different polyoxometalate catalysts in the frame of ultrasound and mixing assisted oxidative desulfurization. *Fuel* **2016**, *180*, 127−136.
(20) Jiang, W.; Jia, H.; Li, H.; Zhu, L.; Tao, R.; Zhu, W.; Li, H.; Dai, S. Boric acid-based ternary deep eutectic solvent for extraction and oxidative desulfurization of diesel fuel. *Green Chem.* **2019**, *21*, 3074−3080.
(21) Gao, S.; Li, J.; Chen, X.; Abdeltawab, A. A.; Yakout, S. M.; Yu, G. A combination desulfurization method for diesel fuel: Oxidation by ionic liquid with extraction by solvent. *Fuel* **2018**, *224*, 545−551.
(22) Verdía, P.; González, E. J.; Rodríguez-Cabo, B.; Tojo, E. Synthesis and characterization of new polysubstituted pyridinium-based ionic liquids: Application as solvents on desulfurization of fuel oils. *Green Chem.* **2011**, *13*, 2768−2776.
(23) Francisco, M.; Arce, A.; Soto, A. Ionic liquids on desulfurization of fuel oils. *Fluid Phase Equilib.* **2010**, *294*, 39−48.
(24) Zhao, D.; Wang, Y.; Duan, E. Oxidative desulfurization of fuel oil by pyridinium-based ionic liquids. *Molecules* **2009**, *14*, 4351−4357.
(25) Enayati, M.; Faghihian, H. *N*-butyl-pyridinium tetrafluoroborate as a highly efficient ionic liquid for removal of dibenzothiophene from organic solutions. *J. Fuel Chem. Technol.* **2015**, *43*, 195−201.
(26) Zhao, D.; Wang, Y.; Duan, E.; Zhang, J. Oxidation desulfurization of fuel using pyridinium-based ionic liquids as phase-transfer catalysts. *Fuel Process. Technol.* **2010**, *91*, 1803−1806.
(27) Nie, Y.; Dong, Y.; Bai, L.; Dong, H.; Zhang, X. Fast oxidative desulfurization of fuel oil using dialkylpyridinium tetrachloroferrates ionic liquids. *Fuel* **2013**, *103*, 997−1002.
(28) Lehn, J.-M. From supramolecular chemistry towards constitutional dynamic chemistry and adaptive chemistry. *Chem. Soc. Rev.* **2007**, *36*, 151−160.
(29) Lehn, J.-M. *Supramolecular Chemistry*; 1st ed.; VCH: Weinheim, 1995.
(30) Hunter, C. A.; Sanders, J. K. The nature of $\pi-\pi$ interactions. *J. Am. Chem. Soc.* **1990**, *112*, 5525−5534.
(31) Zhou, R. The $\pi-\pi$ interactions revisited: Comparison of classical and quantum mechanical calculations. *Modeling of Nanotoxicity*; Springer International Publishing: Switzerland, 2015, 169−189.
(32) González-Rosende, M. E.; Castillo, E.; Jennings, W. B.; Malone, J. F. Stereodynamics and edge-to-face CH$-\pi$ aromatic interactions in imino compounds containing heterocyclic rings. *Org. Biomol. Chem.* **2017**, *15*, 1484−1494.
(33) Hohenstein, E. G.; Sherrill, C. D. Effects of heteroatoms on aromatic π-π interactions: Benzene-pyridine and pyridine dimer. *J. Phys. Chem. A* **2009**, *113*, 878−886.
(34) Frisch, M. J.; et al. *Gaussian 09*; Gaussian, Inc.: Wallingford, CT, 2010.

https://dx.doi.org/10.1021/acsomega.0c00096
ACS Omega 2020, 5, 8023−8031